High-Harmonic Inverse-Free-Electron-Laser Interaction at 800 nm

Christopher M. S. Sears, Eric R. Colby, Benjamin M. Cowan, Robert H. Siemann, and James E. Spencer
Stanford Linear Accelerator Center, Menlo Park, California 94025, USA

Robert L. Byer and Tomas Plettner
Stanford University, Stanford, California 94305, USA
(Received 4 March 2005; published 2 November 2005)

We present the first direct observation of a higher-order inverse-free-electron-laser (IFEL) interaction. Interaction at the fourth, fifth, and sixth harmonics is observed from an IFEL operating at 800 nm. The harmonic spacing, relative harmonic strength, and transverse beam overlap of the interaction are all in good agreement with tracking simulations.

DOI: 10.1103/PhysRevLett.95.194801 PACS numbers: 41.75.Jv, 41.60.Cr

Laser driven accelerators require electron bunches shorter than the laser wavelength. Current rf injectors for linear accelerators have produced electron bunches as short as a few hundred femtoseconds from photocathode guns [1]. This is still much longer than the few femtosecond periods of lasers for acceleration research [2–6]. To obtain net acceleration and increase capture efficiency, previous experiments used an inverse-free electron laser (IFEL) plus a magnetic chicane to microbunch the beam ahead of the accelerator [4,5]. Additionally, it has recently been proposed to use higher harmonic interactions in a multicolor IFEL [5] to further improve bunching. We provide the first direct demonstration of IFEL interaction at higher harmonics and find good agreement with simulation.

An additional important aspect of this research is that we have designed the undulator to operate at 800 nm, near the 1–2 μm region where the most power efficient lasers operate [7] and where accelerator structures made of silicon and silica can be produced by either conventional semiconductor lithography or fiber drawing.

In theory any acceleration scheme can serve as a microbuncher along with a magnetic chicane to turn the energy modulation into a longitudinal density modulation. However, the IFEL has many advantages over other modulation methods. Most conventional accelerator structures require apertures less than or equal to the wavelength, in this case 800 nm. The IFEL, however, has a largely free space interaction with the interaction taking place across the full transverse size of the Gaussian laser beam. To obtain relatively flat phase fronts for the electron microbunching, this spot size is kept fairly large, many hundreds of wavelengths. Additionally, the undulator itself has dimensions that are γ^2 larger than the laser wavelength (a few centimeters for this undulator). This makes fabrication far simpler and simplifies alignment of the electron and laser beams into the IFEL.

The resonance condition for the IFEL interaction is the same as the forward case and given by

$$n = \frac{\lambda_w}{2\lambda_L \gamma^2}\left(1 + \frac{K_w^2}{2}\right), \tag{1}$$

where K_w is the normalized magnetic field of the undulator, λ_w the undulator period, λ_L the laser wavelength, and n the harmonic number [8]. In the case of a simple sinusoidal undulator field and a plane wave laser the electron undergoes a figure-eight motion in the beam frame of reference. Because of the symmetry of the motion, the electron couples only to frequencies at odd harmonics of the oscillation. However, when the electron has an additional net transverse motion the symmetry breaks and the beam can couple to even harmonics of the motion as well [9]. This is the case for the current experiment where the electrons have an additional transverse motion and both beams are undergoing tight focusing inside the undulator. In this experiment the beam energy is half that of the undulator design value to allow resonance over a greater number of harmonics. This beam energy gives the starting harmonic number of $n = 4$. Other harmonics are reached by increasing K_w.

Obtaining analytical results for the amplitude of the interaction at each resonance is more difficult. A solution for a single particle interacting with a plane wave can be found relatively simply, but the geometry of this experiment involves Gaussian beams tightly focused, angular intercepts, and a short undulator in which the nonperiodic end fields cannot be ignored. For this reason, the experiment will instead be compared to simulations that use a simple particle tracker code to propagate a large number of electrons through the undulator in the presence of a Gaussian laser beam. The code integrates the Lorentz equations using the Euler method. A field map of the undulator is loaded from the magnetostatic solver code RADIA [10]. Last, the analytic form for a Gaussian laser beam is included with the static undulator field. Pump depletion and space charge effects are negligible and are not included in the simulation.

TABLE I. IFEL experimental parameters and parameters used in simulation.

Parameter	Value
e-beam energy	30 MeV
e-beam initial energy spread (FWHM)	30 keV (typical)
e-beam charge	2 pC
e-beam pulse length (FWHM)	2 ps
e-beam normalized emittance	2 π-mm-mrad
e-beam focused vertical width (FWHM)	40 μm
e-beam focused horizontal width (FWHM)	210 μm
Laser pulse length (FWHM)	2 ps
Laser wavelength	800 nm
Laser energy	0.5 mJ
Laser focused spot size (FWHM)	110 μm
Undulator period	1.8 cm
Number of periods	3
Strength K_w (adjustable with gap)	0.63–1.7

Table I summarizes the parameters for the IFEL experiment. The laser is synchronized to the accelerator with an additional phase shifter to allow scanning the laser past the e beam in time. Both beams come to a focus in the middle of the undulator (Fig. 1). This increases the peak field of the laser necessary to obtain an appreciable interaction while maintaining good overlap. The beams are aligned using two phosphor screens located at either end of the undulator.

The laser is introduced into the interaction chamber at an angle of $\sim$15 mrad. This eliminates the need for a small chicane to pass the electrons around the last mirror inside the vacuum chamber or a pellicle which would need to be placed far from the focus to avoid laser damage. Also, this experiment was performed in tandem with an inverse transition radiation experiment [11] that requires a laser angle of $\sim 1/\gamma$, or about 15 mrad. To maintain overlap of the electrons and laser inside the undulator along the full electron trajectory, the undulator end fields are detuned so that the electrons move with an angle similar to that of the laser (Fig. 1).

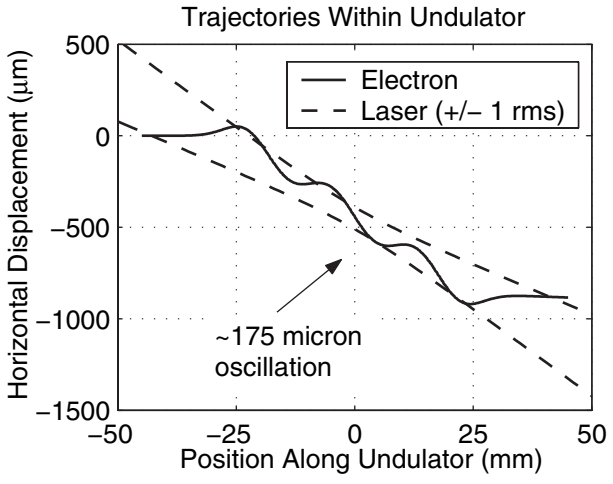

FIG. 1. Calculated trajectory of beam from the measured fields of the undulator. The oscillation increases the horizontal overlap.

The data runs consist of several hundred laser-electron interactions taken at a rate of 10 Hz. Energy spectra are recorded for each electron bunch. For each interaction the offset time between the electron beam and laser is randomly varied over a range of 20–30 ps. In post analysis, the widths of the energy profiles are calculated to determine the energy spread of the electron beam at each shot. Figure 2 shows an example scatter plot of the electron energy spread after the IFEL with the offset time between the two beams. The cross-correlation signal is clear. The width of the cross correlation compared to the known laser pulse length gives an e beam length of $\sim$1 ps. A least squares fit (solid curve) gives a mean interaction for ideal temporal overlap. A number of factors causes spreading of the data under the peak of the interaction, including temporal jitter and electron beam pulse length jitter. To factor out this additional spreading, the maximum interaction (dashed curve) is estimated from the strongest interactions of the peak. Comparison between data runs with the same parameters has found that this peak interaction estimate has a factor of 2 better repeatability between runs compared to the least squares fit amplitude.

In addition to the time offset scan that occurs within every run, between runs other experimental parameters are varied to further explore the IFEL interaction. In particular, the transverse overlap is scanned using a mirror located far

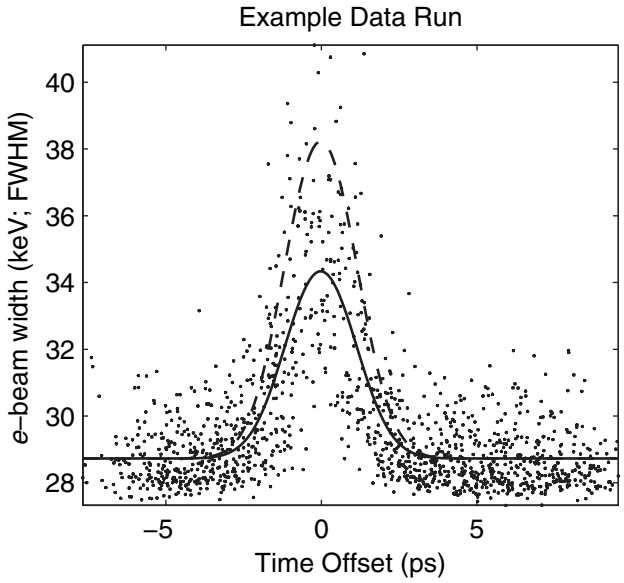

FIG. 2. Example data run with 1500 laser on events. The solid curve is the least squares fit to all data points and gives the mean interaction of 18 keV. The dashed curve is the maximum estimate and gives the peak interaction of 25 keV. The width of cross correlation is 2.2 ps rms.

from the undulator. Also, to observe multiple resonances of the interaction, the gap of the undulator is varied from 4–11 mm.

Results for the horizontal and vertical scans are shown in Fig. 3. While there are just a few runs for each scan, the data do shown good agreement with simulation. The laser waist is known from a knife edge measurement to be 110 μm FWHM. The vertical overlap, which is a cross correlation of the two waists, gives an estimate of the vertical electron beam size of 40 μm FWHM. The horizontal overlap is wider than the vertical overlap due to the transverse oscillations of the electrons through the undulator. At 30 MeV this oscillation is $\sim$175 μm peak to peak (see Fig. 1). Comparison to simulation gives a horizontal spot size of 210 μm FWHM. The asymmetric spot shape is confirmed qualitatively from observations of the spot shape noted at the time of the scan.

It is important to note that neither the data nor simulation in Fig. 3 has been rescaled in energy or offset; the simulation and experiment agree very well for these scans. Within the uncertainty of the runs, we find that 50 keV is the maximum modulation seen for the IFEL interaction. If a chicane were included, this would give a bunching factor of $2b_1 = 0.804$, where b_1 is the ratio of the first Fourier component of the longitudinal density to the average density. The transverse overlap scans were done with the gap set to 6.3 mm, which corresponds to the strongest resonance peak accessible by the experiment.

Compared to the transverse scans the gap scan interaction amplitudes (Fig. 4) are smaller by $\sim$50%. The transverse overlap procedure is accurate to $\sim$25 μm, leaving $\sim$10% uncertainty in the interaction amplitude. Also, there are a number of other parameters that can decrease the interaction amplitude including a larger transverse spot size or longer electron pulse length. Clearly present in the data are two resonances, identified by comparison to Eq. (1) as the fifth and sixth resonances. The fourth order resonance is also clear once it is presented alongside the simulation. While there are a number of data runs around the fourth order peak with small or zero interaction seen, the mean of the data in the range 0.65–0.75 is still well above zero and even slightly above the data from 0.75 to 0.9 indicating a peak. The fourth order peak is also expected from Eq. (1). The simulation also shows additional resonances at larger K_w values; the seventh through ninth resonances, however, the data are too noisy to confirm their presence. While one might expect the fourth resonance to have a stronger interaction due to the lower order, there are two effects that change this. First, the coupling methods for even and odd harmonics are different, and with large crossing angles, higher harmonics can actually have larger coupling strengths [9]. Second, since the alignment is not changed during the gap scan, as the gap increases the laser-electron overlap diminishes. The increase in gap decreases the magnetic field strength, and therefore the electron horizontal motion decreases. This leads to a further roll-off of interaction intensity at large gaps and to a lesser extent as the gap becomes very small (the alignment was done at a gap of 6.3 mm; $K_w = 1$).

Comparison to simulation is complicated by the fact that the overlap diagnostics do not give the absolute position of either beam with respect to the undulator. Therefore, the distance of the electron beam off of the bottom pole tips is not well known. Since the field of an undulator varies as the hyperbolic cosine of the vertical position, the field strength is in turn not well known. However, using the height of the beams as a free parameter in simulation, a best match can be found. Figure 4 gives the best match of simulation to the data where the

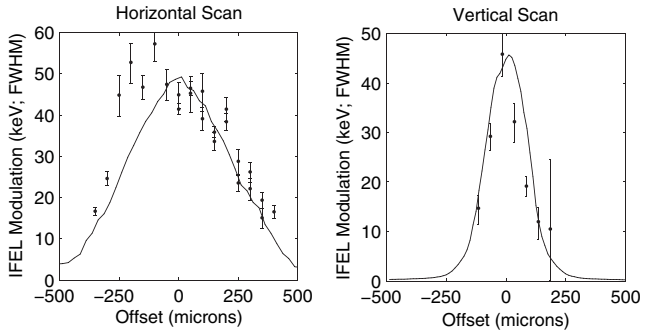

FIG. 3. Vertical and horizontal overlap scans. The solid curve is simulation. The horizontal overlap is wider than the vertical due to the horizontal oscillation of the electrons within the undulator.

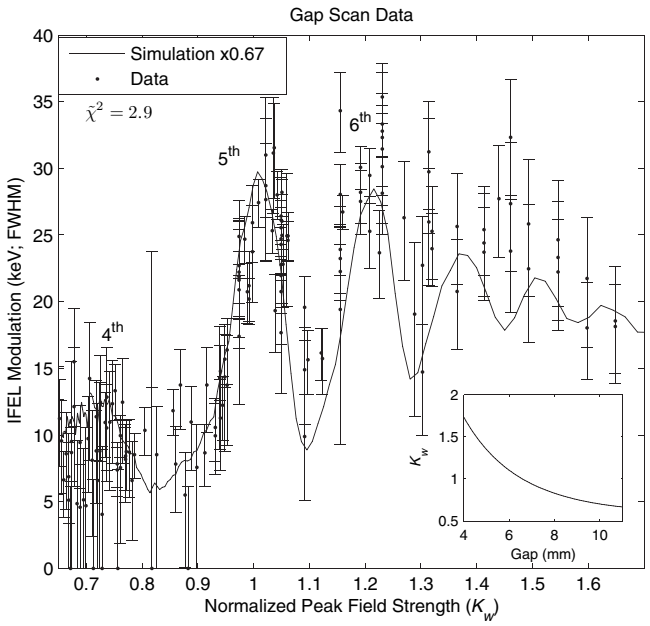

FIG. 4. IFEL gap scan data, with 164 runs total. Comparison to simulation (solid line) shows very good agreement to the shape and spacing of resonance peaks. The harmonic numbers are given next to each peak. Simulation has been rescaled vertically by 0.67 to better visualize overlap.

height of the electrons off of the bottom pole tips is 2.5 mm. The overall amplitude of the simulation is some 50% greater than the raw data, reaching a peak of 50 keV on the fifth harmonic in agreement with the interactions seen during the transverse scans.

With the inclusion of higher harmonics the IFEL can interact over a broad range of parameters. It is worth noting that the fifth and sixth harmonics are comparable in intensity; the IFEL interaction does not necessarily decrease with harmonic number. Both are in fact substantially stronger than the fourth harmonic interaction. With an adjustment of the laser-electron angle the fourth harmonic intensity could also be made stronger. This flexibility extends the utility of undulators or, more simply, aids the experimenter in changing other parameters such as choice of laser wavelength or beam energy.

This experiment has successfully observed harmonic interaction at the fourth through sixth order resonances from an IFEL with an operating wavelength suitable for efficient dielectric laser accelerators. The relative interaction peak amplitudes and spacing agree quite well with simulation. The harmonic interaction could be used in the future to improve bunching via a multicolor IFEL.

The authors would like to thank Roger Carr of Stanford Synchrotron Radiation Laboratory for simulation and design help for the undulator and contribution of materials. We also thank Todd Smith and the staff of HEPL-SCA for their support and Chris Barnes who did the early simulation work on the IFEL. Last, we acknowledge Pietro Musumeci for useful discussions on higher harmonic theory of FELs. This work supported by Department of Energy Contracts No. DE-AC02-76SF00515 and No. DE-FG02-03ER41276.

[1] X. J. Wang *et al.*, Phys. Rev. E **54**, R3121 (1996).
[2] W. D. Kimura *et al.*, Phys. Rev. Lett. **74**, 546 (1995).
[3] K. Nakajima *et al.*, Phys. Rev. Lett. **74**, 4428 (1995).
[4] W. D. Kimura *et al.*, Phys. Rev. ST Accel. Beams **4**, 101301 (2001).
[5] P. Musumeci, C. Pellegrini, and J. B. Rosenzweig, Phys. Rev. E (to be published).
[6] C. D. Barnes, E. R. Colby, and T. Plettner, in *Leap Phase II, Net Energy Gain from Laser Fields in Vacuum*, AIP Conf. Proc. No. 647 (AIP, New York, 2002).
[7] N. V. Kuleshov, A. A. Lagatsky, A. V. Podlinpensky, V. P. Mikhailov, and G. Huber, Opt. Lett. **22**, 1317 (1997).
[8] C. A. Brau, *Free Electron Lasers* (Academic Press, Boston, 1990).
[9] W. B. Colson, G. Dattoli, and F. Ciocci, Phys. Rev. A **31**, 828 (1985).
[10] O. Chubar, P. Elleaume, and J. Chavanne, J. Synchrotron Radiat. **5**, 481 (1998).
[11] T. Plettner *et al.*, Phys. Rev. Lett. **95**, 134801 (2005).